



Cite this: *New J. Chem.*, 2023, **47**, 10826

## Co(II/III), Ni(II) and Cu(II) complexes with a pyrazole-functionalized 1,3,5-triazopentadiene: synthesis, structure and application in the oxidation of styrene to benzaldehyde<sup>†</sup>

Ibadulla Mahmudov,<sup>ab</sup> Atash V. Gurbanov,<sup>\*ac</sup> Luís M. D. R. S. Martins,<sup>\*a</sup> Yusif Abdullayev,<sup>de</sup> Afsun Sujayev,<sup>b</sup> Kamran T. Mahmudov<sup>id, \*ac</sup> and Armando J. L. Pombeiro<sup>ID, a</sup>

A series of coordination compounds  $[\text{Co}^{\text{III}}_2\{(\text{Co}^{\text{II}}\text{Cl}(\text{H}_4\text{L})(\text{H}_2\text{O})_3)_3\}\{(\text{Co}^{\text{II}}(\text{CH}_3\text{COO})(\text{H}_4\text{L})(\text{H}_2\text{O})_2\}_3]^{6+}(\text{Cl}^-)_6\cdot\text{H}_2\text{O}$  (**1**),  $[\text{Ni}(\text{H}_4\text{L})_2]$  (**2**),  $[\text{Cu}(\text{H}_4\text{L})_2]$  (**3**) and  $[(\text{H}_6\text{L})\text{CuCl}_3]\cdot\text{H}_2\text{O}$  (**4**) were synthesized by the reaction of (*E*)-1-(amino(1*H*-pyrazol-1-yl)methylene)guanidinium chloride ( $\text{H}_5\text{L}\text{-HCl}$ ) with  $\text{Co}(\text{CH}_3\text{COO})_2\cdot 4\text{H}_2\text{O}$ ,  $\text{Ni}(\text{CH}_3\text{COO})_2\cdot 4\text{H}_2\text{O}$  (in the presence of triethylamine),  $\text{Cu}(\text{CH}_3\text{COO})_2\cdot \text{H}_2\text{O}$  (in the presence of triethylamine) and  $\text{CuCl}_2\cdot 2\text{H}_2\text{O}$  in methanol, respectively. **1–4** were fully characterized by infrared spectroscopy, electrospray ionization mass spectrometry, single-crystal X-ray diffraction and elemental analyses.  $\text{H}_5\text{L}\text{-HCl}$  is potentially a multidentate *N*-donor ligand, and coordinates to cobalt as a  $\text{N}_4$  donor in **1**, and to nickel or copper as a  $\text{N}_2$  donor in **2–4**. In the structure of **1**, the coordination geometry around the  $\text{Co}^{\text{III}}$  or  $\text{Co}^{\text{II}}$  atoms is distorted octahedral. In **2** and **3**, the Ni and Cu atoms have a distorted square planar coordination geometry, whereas Cu in **4** exhibits a square-based pyramidal coordination geometry. In the packing diagrams of **1–4**, the N atom 1*H*-pyrazole moiety and H–N of the 1,3,5-triazopentadienyl ligands act as a H-bond acceptor and donor towards neighbouring molecules, leading to 3D supramolecular networks. All complexes were tested as catalysts for the peroxidative oxidation of styrene to benzaldehyde. The effects of the oxidant type, styrene to catalyst molar ratio, and reaction temperature and time on the catalytic activity were investigated. Under optimized conditions in the presence of **4**, high yields (up to 80%) of benzaldehyde can be achieved.

Received 9th March 2023,  
Accepted 5th May 2023

DOI: 10.1039/d3nj01120h

rsc.li/njc

## 1. Introduction

The design and synthesis of transition metal complexes of  $\beta$ -diketone,  $\beta$ -diketimine or 1,3,5-triazopentadiene ligands (Scheme 1) have attracted considerable attention because of their magnetic, catalytic, and optical properties.<sup>1</sup> Not only these

synthons (Scheme 1) but also the attached substituents and metal centres can dictate the nuclearity and control the functional and supramolecular properties of their metal complexes. For example, in contrast to mononuclear manganese(II/III) complexes of 1,3,5-triazopentadienyl ligands,<sup>2</sup> due to the participation of the attached 1*H*-pyrazole moiety of (*E*)-1-(amino(1*H*-pyrazol-1-yl)methylene)guanidinium chloride ( $\text{H}_5\text{L}\text{-HCl}$ ) in the coordination, a tetrานuclear Mn(III) complex was obtained, in which the magnetic interaction *via* the imino nitrogen atom in this complex was ferromagnetic.<sup>3</sup> The results of the Cambridge Structural Database search reveal that only two manganese(III) complexes of  $\text{H}_5\text{L}\text{-HCl}$  (Scheme 1) have been reported to date,<sup>3</sup> and our aim herein is to extend the coordination chemistry of this ligand to other transition metals, such as Co(II/III), Ni(II) and Cu(II), and apply them in catalysis. In contrast to transition metal  $\beta$ -diketonates or  $\beta$ -diketiminates, the application of metal complexes of 1,3,5-triazopentadienyl ligands in homogeneous catalysis is comparatively rare.<sup>4</sup> However, the H-bond donor or acceptor sites of  $\text{H}_5\text{L}\text{-HCl}$  (Scheme 1) can make it a good candidate for the construction of multifunctional metal complex catalysts.<sup>5</sup>

<sup>a</sup> Centro de Química Estrutural, Institute of Molecular Sciences, and Departamento de Engenharia Química, Instituto Superior Técnico, Universidade de Lisboa, Av. Rovisco Pais, Lisboa 1049-001, Portugal. E-mail: organik10@hotmail.com, luisammartins@tecnico.ulisboa.pt, kamran.mahmudov@tecnico.ulisboa.pt

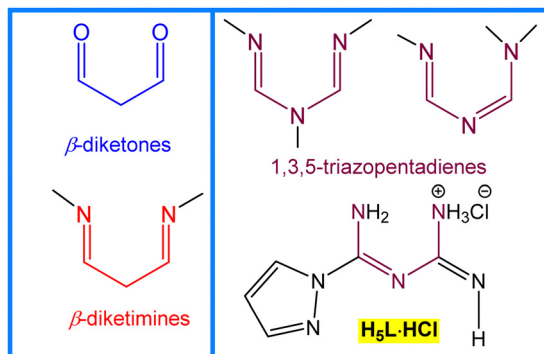
<sup>b</sup> Institute of Chemistry of Additives, Azerbaijan National Academy of Sciences, Baku Az 1029, Azerbaijan

<sup>c</sup> Excellence Center, Baku State University, Z. Xalilov Str. 23, Baku Az 1148, Azerbaijan

<sup>d</sup> Institute of Petrochemical Processes, Azerbaijan National Academy of Sciences, Baku AZ 1025, Azerbaijan

<sup>e</sup> Department of Chemical Engineering, Baku Engineering University, Hasan Aliyev str. 120, Absheron, Baku, AZ 0101, Azerbaijan

<sup>†</sup> Electronic supplementary information (ESI) available. CCDC 2193859–2193862. For ESI and crystallographic data in CIF or other electronic format see DOI: <https://doi.org/10.1039/d3nj01120h>

Scheme 1 Schematic illustration of  $\beta$ -diketones and  $N$ -ligands.

Among the many modern functionalization procedures, the selective oxidation of alkenes to the corresponding aldehydes concerns one of the important synthetic strategies in homogenous catalysis.<sup>6</sup> The resulting aldehydes are versatile intermediates in the synthesis of fine chemicals and have applications in dyestuff, perfumery, and food processing industries, etc. Currently, two main synthetic procedures are used in the industrial production of benzaldehyde: (i) hydrolysis of benzal chloride; and (ii) catalytic oxidation of toluene to benzaldehyde with oxygen.<sup>7</sup> However, both methods have several disadvantages, such as low yield (up to 20%), long reaction time, high temperature, poor selectivity, production of chloride wastes, etc.<sup>8</sup> Therefore, the search for a new effective, inexpensive and environmentally friendly catalytic system remains a serious challenge in both academic and industrial fields because of the significance of benzaldehyde, and the lack of selectivity of the present processes.

Various classes of organic ligands have already been examined in the metal complex catalyzed oxidation of styrene to benzaldehyde<sup>9</sup> but, to our knowledge, 1,3,5-triazopentadienyl ligands have not yet been reported for such a purpose. Moreover, the use of hydrogen peroxide as the oxygen source constitutes a sustainable strategy to perform homogenous catalytic transformations.<sup>10</sup>

Considering all the above points, this work pursued the following objectives: (i) to synthesize  $\text{Co}(\text{II/III})$ ,  $\text{Ni}(\text{II})$  and  $\text{Cu}(\text{II})$  complexes of (*E*)-1-(amino(1*H*-pyrazol-1-yl)methylene)guanidinium chloride ( $\text{H}_5\text{L}\cdot\text{HCl}$ ); (ii) to apply the obtained transition metal 1,3,5-triazopentadienates as catalysts or catalyst precursors for the peroxidative oxidation of styrene to benzaldehyde under mild conditions.

## 2. Results and discussion

### 2.1. Synthesis and characterization of $\text{H}_5\text{L}\cdot\text{HCl}$ and **1–4**

The synthesis and characterization of (*E*)-1-(amino(1*H*-pyrazol-1-yl)methylene)guanidinium chloride ( $\text{H}_5\text{L}\cdot\text{HCl}$ ) was reported earlier,<sup>3</sup> and will not be discussed herein. Four new transition metal 1,3,5-triazopentadienates,  $[\text{Co}^{\text{III}}_2\{(\text{Co}^{\text{II}}\text{Cl}(\text{H}_4\text{L})(\text{H}_2\text{O})_3)_3\}\cdot\{(\text{Co}^{\text{II}}(\text{CH}_3\text{COO})(\text{H}_4\text{L})(\text{H}_2\text{O})_2\}_3]^{6+}(\text{Cl}^-)_6\cdot\text{H}_2\text{O}$  (**1**),  $[\text{Ni}(\text{H}_4\text{L})_2]$  (**2**),  $[\text{Cu}(\text{H}_4\text{L})_2]$  (**3**) and  $[(\text{H}_6\text{L})\text{CuCl}_3]\cdot\text{H}_2\text{O}$  (**4**), were synthesized by

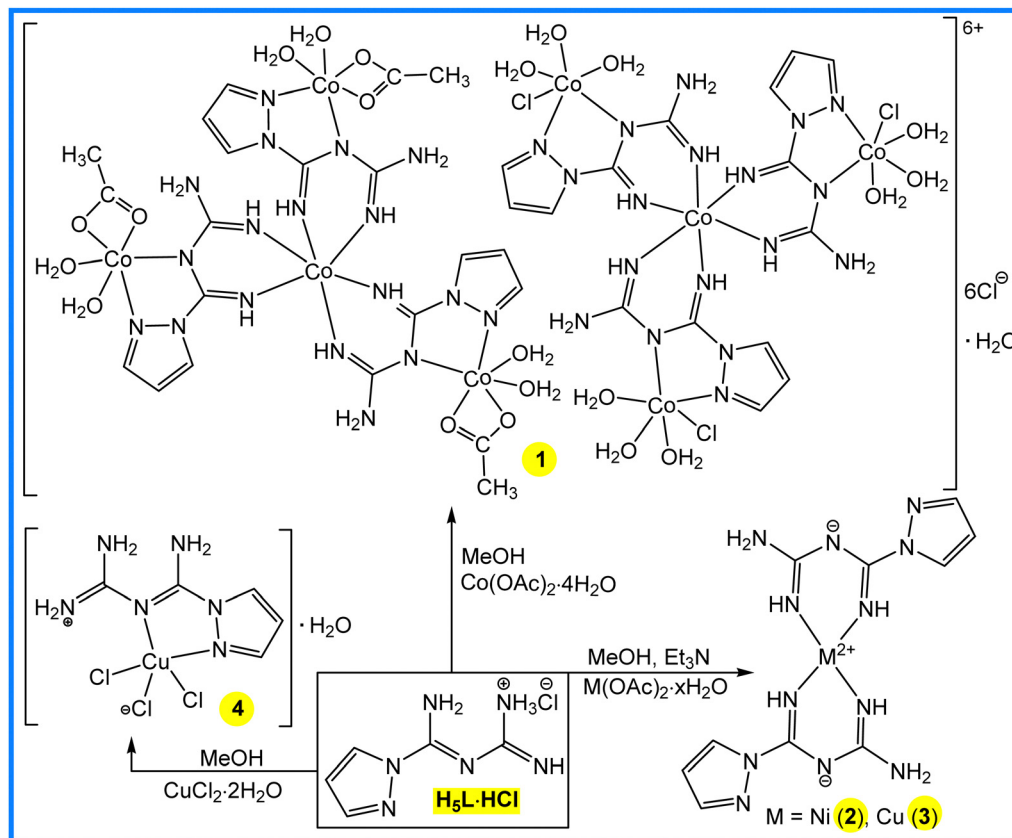
the reaction of  $\text{H}_5\text{L}\cdot\text{HCl}$  with  $\text{Co}(\text{CH}_3\text{COO})_2\cdot 4\text{H}_2\text{O}$ ,  $\text{Ni}(\text{CH}_3\text{COO})_2\cdot 4\text{H}_2\text{O}$  (in the presence of triethylamine),  $\text{Cu}(\text{CH}_3\text{COO})_2\cdot \text{H}_2\text{O}$  (in the presence of triethylamine) and  $\text{CuCl}_2\cdot 2\text{H}_2\text{O}$  in methanol, respectively (Scheme 2).

In the IR spectra of **1**, **2**, **3** and **4**, broad and strong  $\nu(\text{N}-\text{H})$  bands appear at 2952, 3347, 3377 and  $3217\text{ cm}^{-1}$ , whereas the  $\nu(\text{C}=\text{N})$  absorption bands occur at 1587, 1595, 1592 and  $1651\text{ cm}^{-1}$ , respectively, and are significantly shifted in comparison to the corresponding peak of  $\text{H}_5\text{L}\cdot\text{HCl}$  ( $1646\text{ cm}^{-1}$ ).<sup>3</sup> There is no strong absorption signal around  $1700\text{ cm}^{-1}$  for  $-\text{COOH}$  in the IR spectrum of **1**, indicating that the carboxylate group of the acetate is participating in coordination ( $1623\text{ cm}^{-1}$ ). The following ESI-MS peaks were observed:  $324.7\text{ [Co}^{\text{III}}\{(\text{Co}^{\text{II}}(\text{CH}_3\text{COO})(\text{H}_4\text{L})(\text{H}_2\text{O})_2\}_3\}]^{3+}$ ,  $318.6\text{ [Co}^{\text{III}}\{(\text{Co}^{\text{II}}\text{Cl}(\text{H}_4\text{L})(\text{H}_2\text{O})_3\}_3\}]^{3+}$  and  $34.9\text{ Cl}^-$  (for **1**),  $362.1\text{ [Ni}(\text{H}_4\text{L})_2\text{] + H}^+$  (for **2**),  $366.8\text{ [Cu}(\text{H}_4\text{L})_2\text{] + H}^+$  (for **3**) and  $324.1\text{ [(\text{H}_6\text{L})\text{CuCl}_3]\cdot\text{H}_2\text{O} + H}^+$  (for **4**). A strong absorption band from 283 to  $312\text{ nm}$  and a weak absorption band from 418 to  $481\text{ nm}$  were observed in the UV/Vis spectra of **1–4** in acetonitrile solution. Elemental analyses and X-ray crystallography (Scheme 2 and Fig. 1) are also in agreement with the proposed formulations.

In the crystal, the unit cell of the complex **1** is composed of the two  $[\text{Co}^{\text{III}}\{(\text{Co}^{\text{II}}(\text{CH}_3\text{COO})(\text{H}_4\text{L})(\text{H}_2\text{O})_2\}_3\}]^{3+}$  and  $[\text{Co}^{\text{III}}\{(\text{Co}^{\text{II}}\text{Cl}(\text{H}_4\text{L})(\text{H}_2\text{O})_3\}_3\}]^{3+}$  tetranuclear complex cations, six  $\text{Cl}^-$  anions and a water molecule. In both cations, the central  $\text{Co}^{3+}$  ion has a distorted octahedral coordination environment with six nitrogen donors from three bidentate 1,3,5-triazopentadienyl ligands. In the  $[\text{Co}^{\text{III}}\{(\text{Co}^{\text{II}}(\text{CH}_3\text{COO})(\text{H}_4\text{L})(\text{H}_2\text{O})_2\}_3\}]^{3+}$  cation, each  $\text{Co}^{2+}$  centre shows a slightly distorted octahedral  $\text{CoN}_2\text{O}_4$  coordination environment with ligation from two carboxylate O atoms from the acetate ligand, two N atoms from the 1,3,5-triazopentadienyl ligand and two O atoms from water molecules. Similarly, in the  $[\text{Co}^{\text{III}}\{(\text{Co}^{\text{II}}\text{Cl}(\text{H}_4\text{L})(\text{H}_2\text{O})_3\}_3\}]^{3+}$  cation, the  $\text{Co}^{\text{II}}$  centre also appears to be octahedrally coordinated by two nitrogen atoms from the 1,3,5-triazopentadienyl ligand, one chloride atom and three water molecules. In the packing arrangement, the coordinated 1,3,5-triazopentadienyl and chloride ligands, water molecules and chloride anions are involved in intermolecular noncovalent interactions to form a 3D supramolecular framework (Fig. S1, ESI<sup>†</sup>).

Complexes **2** and **3** are isostructural (Scheme 2 and Fig. 1). The metal center possesses a distorted square planar geometry in **2** ( $\tau_4 = 0$ ) and **3** ( $\tau_4 = 0$ ),<sup>11</sup> coordinated by the imino nitrogen atoms of two uninegatively charged 1,3,5-triazopentadienyl ligands. In the six-membered planar metallacycles in both complexes, the  $\text{C}=\text{N}$  imine bond distances ( $1.297\text{--}1.321\text{ \AA}$ ) are within the range of typical  $\text{C}=\text{N}$  bond lengths in relevant metal<sup>II</sup>-*bis*-1,3,5-triazapentadienates,<sup>1c</sup> which indicates a high delocalization within the  $\text{N}=\text{C}-\text{N}^--\text{C}=\text{N}$  moiety. The 1*H*-pyrazolyl arms are bending out of the metallacycle plane, but act as H-bond acceptors in intermolecular interactions in the crystal packing of **2** and **3** (Fig. S2 and S3, ESI<sup>†</sup>). Both structures are further stabilized by weak intermolecular H-bonding interactions involving the NH (as the H-bond donor) and  $\text{N}^-$  (as the H-bond acceptor) of 1,3,5-triazopentadienyl ligands (Fig. S2 and S3, ESI<sup>†</sup>).



Scheme 2 Synthesis of **1–4**.

In **4**, the copper atom is pentacoordinated with a square-based pyramidal coordination geometry ( $\tau_5 = 0.17$ ) (Scheme 2 and Fig. 1). The square plane is defined by the more strongly bonded Cl1 (2.251 Å) and Cl2 (2.231 Å) and two nitrogen (Cu1–N1 1.985 and Cu1–N3 2.065 Å) atoms of the bidentate 1,3,5-triazopentadienyl ligand, and the apical position is occupied by the Cl3 (2.784 Å) (Fig. 1), which reflects the weak axial interactions as expected for Jahn–Teller distorted copper(II) complexes.<sup>11</sup> The free imide nitrogen is protonated, so that the overall complex is neutral. In **4** all coordinated chlorine atoms act as hydrogen bond acceptors towards H–N of the 1,3,5-triazopentadienyl ligands (Fig. S4, ESI†), with the N–H $\cdots$ Cl distance of 3.13–3.23 Å. Moreover, hydrate water molecule acts as a H-bond donor or acceptor towards coordinated chlorine atoms (3.22 and 3.24 Å) or the H–N moiety of the 1,3,5-triazopentadienyl ligands (2.81 Å), respectively, building up an intricate 3D network (Fig. S4, ESI†).

## 2.2. Catalytic activity of **1–4** in the peroxidative oxidation of styrene to benzaldehyde

The catalytic activity of complexes **1–4** for the peroxidative oxidation of styrene to benzaldehyde was evaluated (Scheme 3). In general, styrene, catalyst, oxidant and solvent were included in a sealed tube reactor and heated to the desired temperature and time. Selected results are collected in Table 1.

The reaction was performed in acetonitrile owing to its high resistance to oxidizing agents, solubility of the catalysts and substrate, miscibility with water and viscosity. No oxidation reaction between styrene and H<sub>2</sub>O<sub>2</sub> takes place in acetonitrile in the absence of catalysts **1–4**, but in the presence of Co(CH<sub>3</sub>COO)<sub>2</sub>·4H<sub>2</sub>O, Ni(CH<sub>3</sub>COO)<sub>2</sub>·4H<sub>2</sub>O, Cu(CH<sub>3</sub>COO)<sub>2</sub>·H<sub>2</sub>O or CuCl<sub>2</sub>·2H<sub>2</sub>O, benzaldehyde was produced in 5.8–10.6% yield (entries 1–5, Table 1).

The possibility of using solvent-free conditions was also tested but without success (entries 10–13, Table 1). Aiming at reaching the optimal reaction conditions to achieve the maximum selective formation of benzaldehyde, the effects of the oxidant type, styrene to catalyst molar ratio, and reaction time and temperature on the catalytic activity of **1–4** were investigated.

The effect of using the same molar amount of *tert*-butyl hydroperoxide (TBHP, 70 wt% aq.) or hydrogen peroxide (H<sub>2</sub>O<sub>2</sub>, 30 wt% aq.) as oxygen sources in the styrene oxidation reaction was studied, maintaining the remaining reaction conditions. The results (Table 1) indicated that while only a maximum of 36% of selectivity to benzaldehyde formation was achieved when TBHP was used as the oxidant (entry 17, Table 1, for catalyst **4**), it reached 96% when H<sub>2</sub>O<sub>2</sub> was used, accompanied by a yield of 80% (under the best reaction conditions, entry 9, Table 1, for catalyst **4**). Therefore, hydrogen peroxide is the optimal oxidant for this catalytic system for the oxidation of

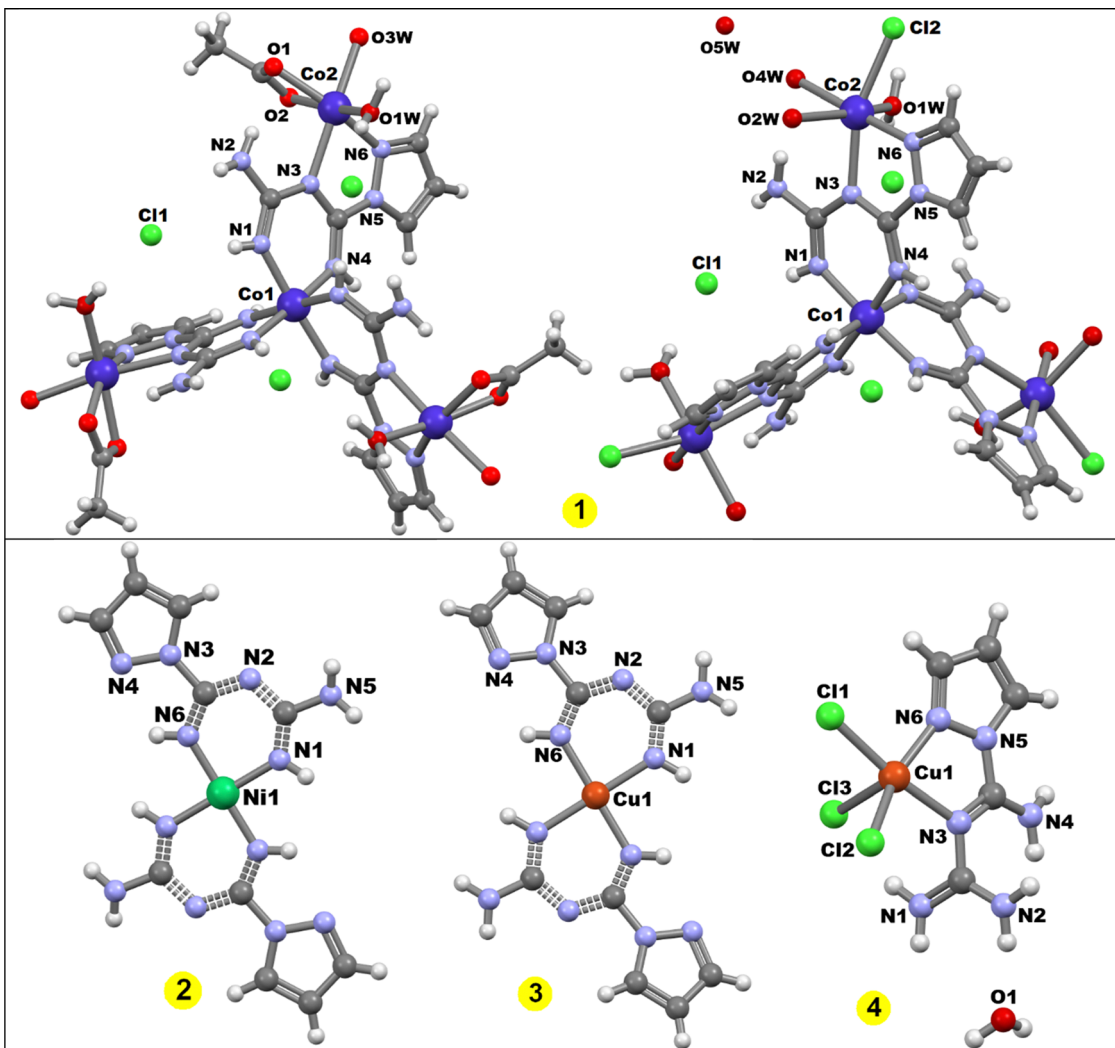
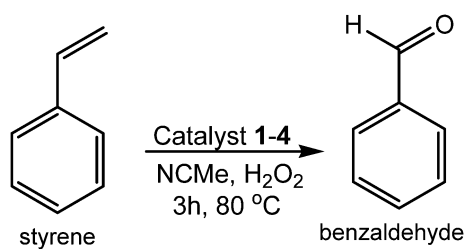


Fig. 1 Crystal structures of **1–4** with a partial atom numbering scheme. In the structure of **1**, H atoms of O2w, O3w, O4w and O5w were not located.



Scheme 3 Peroxidative oxidation of styrene to benzaldehyde catalysed by **1–4**.

styrene to benzaldehyde, minimizing the amounts of styrene oxide, 1-phenylethane-1,2-diol and benzoic acid (undesired side products).

Reaction temperature was found to be a crucial factor as it significantly impacted the styrene conversion (compare entries 6–9 to 18–21, Table 1). The same applies to the reaction time (compare entries 6–9 to 22–26, Table 1). Thus, the best conditions found for catalysts **1–4** were 3 h of heating at 80 °C

(entries 6–9, Table 1). An increase of the catalyst amount in the reaction medium, which would impact the catalytic system cost, revealed to be detrimental for selectivity, although leading to an increase of the conversion (entries 26–29, Table 1) and 5 µmol per mmol of styrene was determined to be the optimal amount for its catalytic oxidation in the presence of **1–4**. The undesired by-product benzoic acid was formed at higher temperatures and longer reaction times or in the presence of a stronger oxidant, TBHP, suggesting that it was a product of oxidation of the formed aldehyde. Under such conditions, very small amounts (<5%) of 1-phenylethane-1,2-diol and 2-hydroxy-1-phenylethanone (resulting from oxidation of the diol) could also be observed. In contrast, styrene epoxide was detected for milder or shorter reaction times, in accordance with its proposed role as an intermediate in the formation of the aldehyde.<sup>8,12,13</sup>

As presented in Table 1, the best catalytic results were obtained with the Cu(II) catalysts, complex **4** being the best catalyst for the selective conversion of styrene into benzaldehyde.

Table 1 Effect of the reaction conditions on the catalytic activity of complexes **1–4** (selected results)

Entry	Catalyst	Solvent	Oxidant	T/°C	t/h	n (styrene)/n (cat)	Yield <sup>a</sup> /%	Conversion/%
1	—	NCMe	H <sub>2</sub> O <sub>2</sub>	80	3	1 mmol/5 µmol	—	—
2	Co(CH <sub>3</sub> COO) <sub>2</sub> ·4H <sub>2</sub> O	NCMe	H <sub>2</sub> O <sub>2</sub>	80	3	1 mmol/5 µmol	6.9	33
3	Ni(CH <sub>3</sub> COO) <sub>2</sub> ·4H <sub>2</sub> O	NCMe	H <sub>2</sub> O <sub>2</sub>	80	3	1 mmol/5 µmol	5.8	17
4	Cu(CH <sub>3</sub> COO) <sub>2</sub> ·H <sub>2</sub> O	NCMe	H <sub>2</sub> O <sub>2</sub>	80	3	1 mmol/5 µmol	10.6	56
5	CuCl <sub>2</sub> ·2H <sub>2</sub> O	NCMe	H <sub>2</sub> O <sub>2</sub>	80	3	1 mmol/5 µmol	9.4	47
6	1	NCMe	H <sub>2</sub> O <sub>2</sub>	80	3	1 mmol/5 µmol	39.6	99
7	2	—	H <sub>2</sub> O <sub>2</sub>	80	3	1 mmol/5 µmol	37.1	57
8	3	—	H <sub>2</sub> O <sub>2</sub>	80	3	1 mmol/5 µmol	57.0	77
9	4	—	H <sub>2</sub> O <sub>2</sub>	80	3	1 mmol/5 µmol	80.0	83
10	1	—	H <sub>2</sub> O <sub>2</sub>	80	3	1 mmol/5 µmol	2.0	6
11	2	—	H <sub>2</sub> O <sub>2</sub>	80	3	1 mmol/5 µmol	3.6	18
12	3	—	H <sub>2</sub> O <sub>2</sub>	80	3	1 mmol/5 µmol	11.0	22
13	4	—	H <sub>2</sub> O <sub>2</sub>	80	3	1 mmol/5 µmol	16.4	26
14	1	NCMe	TBHP	80	3	1 mmol/5 µmol	16.0	>99
15	2	NCMe	TBHP	80	3	1 mmol/5 µmol	14.4	72
16	3	NCMe	TBHP	80	3	1 mmol/5 µmol	19.1	91
17	4	NCMe	TBHP	80	3	1 mmol/5 µmol	35.3	98
18	1	NCMe	H <sub>2</sub> O <sub>2</sub>	60	3	1 mmol/5 µmol	21.5	50
19	2	NCMe	H <sub>2</sub> O <sub>2</sub>	60	3	1 mmol/5 µmol	17.6	27
20	3	NCMe	H <sub>2</sub> O <sub>2</sub>	60	3	1 mmol/5 µmol	29.1	41
21	4	NCMe	H <sub>2</sub> O <sub>2</sub>	60	3	1 mmol/5 µmol	39.2	40
22	1	NCMe	H <sub>2</sub> O <sub>2</sub>	80	2	1 mmol/5 µmol	23.0	64
23	2	NCMe	H <sub>2</sub> O <sub>2</sub>	80	2	1 mmol/5 µmol	19.8	33
24	3	NCMe	H <sub>2</sub> O <sub>2</sub>	80	2	1 mmol/5 µmol	45.8	52
25	4	NCMe	H <sub>2</sub> O <sub>2</sub>	80	2	1 mmol/5 µmol	53.4	58
26	1	NCMe	H <sub>2</sub> O <sub>2</sub>	80	3	1 mmol/10 µmol	19.0	>99
27	2	NCMe	H <sub>2</sub> O <sub>2</sub>	80	3	1 mmol/10 µmol	23.0	72
28	3	NCMe	H <sub>2</sub> O <sub>2</sub>	80	3	1 mmol/10 µmol	37.4	89
29	4	NCMe	H <sub>2</sub> O <sub>2</sub>	80	3	1 mmol/10 µmol	43.7	93

<sup>a</sup> values calculated from GC analysis (internal standard method).

Both the reaction time (3 h) and selectivity (96%, entry 9 in Table 1) in our system are usually higher than those reported for  $[\text{Ni}(\text{L}^1\text{NHC})_2](\text{PF}_6)_2$ , ( $\text{L}^1\text{NHC} = (E)\text{-3-methyl-1-propyl-4-(2-((2-(pyridin-2-yl)ethyl)imino)methyl)phenyl-1H-1,2,3-triazol-3-ium}$  hexafluorophosphate(V) (reaction time 6 h, selectivity 70%)<sup>14</sup> and  $[\text{2-ampH}]_4[\{\text{Co}(\text{H}_2\text{O})_5\}\text{Mo}_7\text{O}_{24}]\cdot 9\text{H}_2\text{O}$ , (2-amp = 2-aminopyridine), (reaction time 24 h, selectivity 76%)<sup>15</sup> complexes.

### 3. Conclusions

In this work we have successfully used a 1,3,5-triazopentadienyl chelating ligand bearing a 1*H*-pyrazol fragment to synthesize novel tetranuclear Co(II/III) (**1**) and mononuclear Ni(II) (**2**) and Cu(II) (**3** and **4**) complexes. Unlike most cases in which a metal ion is coordinated by both imine nitrogen atoms of 1,3,5-triazopentadienyls, the cobalt and copper (in **4**) ions are coordinated by one 1*H*-pyrazole nitrogen atom and the central nitrogen atom of the 1,3,5-triazopentadienyl ring. The coordination environment and the supramolecular chemistry of the obtained complexes are dependent on the nature of metal atoms and on the reaction conditions.

In comparison with the tetranuclear Co(II/III) (**1**) and mononuclear Ni(II) (**2**) complexes, both Cu(II) (**3** and **4**) complexes act as more selective catalysts in the peroxidative conversion of styrene into benzaldehyde. A good catalytic activity is observed in the use of H<sub>2</sub>O<sub>2</sub> and acetonitrile instead of TBHP and solvent-free conditions. The higher catalytic activity of compound **4** in

comparison with that of **3** can be consistent with the presence of chloride labile ligands which can undergo easy displacement and eventually accelerate this synthetic transformation.

## 4. Experimental

### 4.1. Materials and instrumentation

All the chemicals were obtained from commercial sources and used as received. (E)-1-(amino(1*H*-pyrazol-1-yl)methylene) guanidinium chloride (H<sub>5</sub>L·HCl) was synthesized according to a reported synthetic procedure.<sup>3</sup> The IR spectra (4000–400 cm<sup>-1</sup>) were recorded on a Bruker Alpha-P ATR-IR spectrometer. Carbon, hydrogen and nitrogen elemental analyses were carried out using the Microanalytical Service of the Instituto Superior Técnico. Electrospray mass spectra (ESI-MS) were run with an ion-trap instrument (Varian 500-MS LC ion trap mass spectrometer) equipped with an electrospray ion source. For electrospray ionization, the drying gas and flow rate were optimized according to the particular sample with a 35 p.s.i. nebulizer pressure. Scanning was performed from *m/z* 10 to 2000 in methanol solution. The compounds were observed in the positive or negative ion mode (capillary voltage = 80–105 V). The UV-vis absorption spectra in the 200–700 nm region were recorded with a scan rate of 240 nm min<sup>-1</sup> by using a Lambda 35 UV-vis spectrophotometer (PerkinElmer) in 1.00 cm quartz cells at room temperature, with a concentration of **1–4** of  $1.00 \times 10^{-6}$  mol L<sup>-1</sup> in acetonitrile.



## 4.2. Synthesis of complexes

**Synthesis of 1.**  $\text{H}_5\text{L}\cdot\text{HCl}$  (188 mg, 1 mmol) was dissolved in 20 mL of methanol and  $\text{Co}(\text{CH}_3\text{COO})_2\cdot 4\text{H}_2\text{O}$  (249 mg, 1 mmol) was added. The obtained orange solution was stirred for 10 min and then left in open air at room temperature for slow evaporation to afford **1** as orange crystals suitable for X-ray measurements.

$[\text{Co}^{\text{III}}_2\{\text{Co}^{\text{II}}\text{Cl}(\text{H}_4\text{L})(\text{H}_2\text{O})_3\}_3\{\text{Co}^{\text{II}}(\text{CH}_3\text{COO})(\text{H}_4\text{L})(\text{H}_2\text{O})_2\}_3]^{6+}\cdot(\text{Cl}^-)_6\cdot\text{H}_2\text{O}$  (**1**): yield, 57% (based on Co). Orange crystalline compound soluble in methanol, ethanol and DMF. Elemental analysis, anal. calcd. (%) for  $\text{C}_{36}\text{H}_{63}\text{Cl}_9\text{Co}_8\text{N}_{36}\text{O}_{22}$  ( $Mr = 2162.81 \text{ g mol}^{-1}$ ): C 19.99, H 3.87, N 23.31. Found: C 20.11, H 3.76, N 23.47. ESI-MS:  $m/z$ : 324.7  $[\text{Co}^{\text{III}}\{\text{Co}^{\text{II}}(\text{CH}_3\text{COO})(\text{H}_4\text{L})(\text{H}_2\text{O})_2\}_3]^{3+}$ , 318.6  $[\text{Co}^{\text{III}}\{\text{Co}^{\text{II}}\text{Cl}(\text{H}_4\text{L})(\text{H}_2\text{O})_3\}_3]^{3+}$  and 34.9  $\text{Cl}^-$ . IR (KBr, selected bands,  $\text{cm}^{-1}$ ): 3276  $\nu(\text{O}-\text{H})$ , 2952  $\nu(\text{N}-\text{H})$ , 1623  $\nu(\text{C}=\text{O})$  and 1587  $\nu(\text{C}=\text{N})$ .  $\lambda^{\text{abs}}/\text{nm}$ : 312 and 481.

**Synthesis of 2 and 3.**  $\text{H}_5\text{L}\cdot\text{HCl}$  (188 mg, 1 mmol) was dissolved in 20 mL of methanol, then 2 drops of triethylamine and  $\text{Ni}(\text{CH}_3\text{COO})_2\cdot 4\text{H}_2\text{O}$  (125 mg, 0.5 mmol) or  $\text{Cu}(\text{CH}_3\text{COO})_2\cdot \text{H}_2\text{O}$  (100 mg, 0.5 mmol) were added. The reaction mixture was stirred for 10 min and then left in open air at room temperature for slow evaporation to yield **2** or **3** as orange or pink crystals, respectively, suitable for X-ray analysis.

$[\text{Ni}(\text{H}_4\text{L})_2]$  (**2**): yield, 68% (based on Ni). Orange crystalline compound soluble in methanol, ethanol and DMF. Elemental analysis, anal. calcd. (%) for  $\text{C}_{10}\text{H}_{14}\text{N}_{12}\text{Ni}$  ( $Mr = 361.0 \text{ g mol}^{-1}$ ): C 33.27, H 3.91, N 46.56. Found: C 33.21, H 3.87, N 46.41. ESI-MS:  $m/z$ : 362.1 [ $Mr + \text{H}^+$ ]. IR (KBr, selected bands,  $\text{cm}^{-1}$ ): 3347  $\nu(\text{N}-\text{H})$  and 1595  $\nu(\text{C}=\text{N})$ .  $\lambda^{\text{abs}}/\text{nm}$ : 295 and 448.

$[\text{Cu}(\text{H}_4\text{L})_2]$  (**3**): yield, 77% (based on Cu). Pink crystalline compound soluble in methanol, ethanol and DMF. Elemental analysis, anal. calcd. (%) for  $\text{C}_{10}\text{H}_{14}\text{CuN}_{12}$  ( $Mr = 365.8 \text{ g mol}^{-1}$ ): C 32.83, H 3.86, N 45.94. Found: C 33.79, H 3.85, N 45.90. ESI-MS:  $m/z$ : 366.8 [ $Mr + \text{H}^+$ ]. IR (KBr, selected bands,  $\text{cm}^{-1}$ ): 3377  $\nu(\text{N}-\text{H})$  and 1592  $\nu(\text{C}=\text{N})$ .  $\lambda^{\text{abs}}/\text{nm}$ : 299 and 453.

**Synthesis of 4.**  $\text{H}_5\text{L}\cdot\text{HCl}$  (188 mg, 1 mmol) was dissolved in 20 mL of methanol, then  $\text{CuCl}_2\cdot 2\text{H}_2\text{O}$  (170 mg, 1 mmol) was added and the system was stirred for 10 min. After *ca.* 2 d at room temperature, green crystals precipitated and were filtered off and dried in air.

$[(\text{H}_5\text{L})\text{CuCl}_3]$  (**4**): yield, 80% (based on Cu). Green crystalline compound soluble in methanol, ethanol and DMF. Elemental analysis, anal. calcd. (%) for  $\text{C}_{5}\text{H}_{11}\text{Cl}_3\text{CuN}_6\text{O}$  ( $Mr = 341.1 \text{ g mol}^{-1}$ ): C 17.61, H 3.25, N 24.64. Found: C 17.58, H 3.21, N 24.60. ESI-MS:  $m/z$ : 324.1 [ $Mr - \text{H}_2\text{O} + \text{H}^+$ ]. IR (KBr, selected bands,  $\text{cm}^{-1}$ ): 3582 and 3466  $\nu(\text{O}-\text{H})$ , 3217 and 3038  $\nu(\text{N}-\text{H})$  and 1651  $\nu(\text{C}=\text{N})$ .  $\lambda^{\text{abs}}/\text{nm}$ : 283 and 418.

## 4.3. X-ray structure determinations

X-ray diffraction intensities of compounds **1–4** were collected using a BRUKER D8 QUEST diffractometer (graphite-monochromated radiation  $\text{Mo K}\alpha$ ,  $\lambda = 0.71073 \text{ \AA}$ ) at 150(2) K. An absorption correction was applied to all data using the program SADABS.<sup>16,17</sup> All the structures were solved by direct methods and refined on  $F^2$  by full-matrix least-squares using Bruker's SHELXTL-97.<sup>18</sup> All non-hydrogen atoms were refined anisotropically.

In complex **1** a disordered coordination sphere was detected about  $\text{Co}_2$  (an acetate anion and a water molecule are replaced by a chloride and two water molecules, all at half occupancy). H atoms of all these water molecules were not located as well as those of a lattice water molecule (Ow5), detected in the difference Fourier and refined with an occupancy of 0.5. In addition in complex **1** a potential solvent area of  $758.3 \text{ \AA}^3$  [15.9% of unit cell] is present and the Squeeze tool<sup>19</sup> was used to take into account the contribution of disordered solvent in **1**.

The details of the crystallographic data for complexes **1–4** are summarized in Table 2. CCDC 2193859 (for **1**), 2193862 (2), 2193861 (3) and 2193860 (4) contains the supplementary crystallographic data for this paper.

Table 2 Crystallographic data and structure refinement details for **1–4**

Empirical formula	<b>1</b> $\text{C}_{36}\text{H}_{63}\text{Cl}_9\text{Co}_8\text{N}_{36}\text{O}_{22}$	<b>2</b> $\text{C}_{10}\text{H}_{14}\text{N}_{12}\text{Ni}$	<b>3</b> $\text{C}_{10}\text{H}_{14}\text{CuN}_{12}$	<b>4</b> $\text{C}_{5}\text{H}_{11}\text{Cl}_3\text{CuN}_6\text{O}$
fw	2142.71	361.04	365.87	341.09
Temperature (K)	150(2)	150(2)	150(2)	150(2)
Cryst. syst.	Trigonal	Monoclinic	Triclinic	Monoclinic
Space group	$P\bar{3}1c$	$P2_1/c$	$\bar{P}1$	$C2/c$
$a$ (Å)	16.4531(6)	12.2955(8)	8.1733(4)	24.4255(4)
$b$ (Å)	16.4531(6)	4.9045(3)	9.3238(5)	8.71870(10)
$c$ (Å)	20.2962(13)	13.1699(9)	15.0254(8)	13.6691(3)
$\alpha$ (°)	90	90	76.085(2)	90
$\beta$ (°)	90	116.167(2)	77.688(2)	123.7980(10)
$\gamma$ (°)	120	90	80.873(2)	90
$V$ (Å <sup>3</sup> )	4758.2(5)	712.79(8)	1078.89(10)	2419.01(8)
$Z$	2	2	3	8
$\rho_{\text{calc}}$ (g cm <sup>-3</sup> )	1.484	1.682	1.689	1.873
$\mu$ (Mo $\text{K}\alpha$ ) (mm <sup>-1</sup> )	1.682	1.383	1.540	2.457
$F(000)$	2136	372	561	1368
$R_1^a$ [ $I \geq 2\sigma$ ]	0.0737	0.0205	0.0259	0.0167
$wR_2^b$ [ $I \geq 2\sigma$ ]	0.2037	0.0473	0.0684	0.0461
GOOF	1.064	1.071	1.056	1.104

<sup>a</sup>  $R_1 = \sum ||F_{\text{o}}|| - |F_{\text{c}}|| / \sum |F_{\text{o}}||$ . <sup>b</sup>  $wR_2 = [\sum w(F_{\text{o}}^2 - F_{\text{c}}^2)^2] / \sum w(F_{\text{o}}^2)^2]^{1/2}$ .



#### 4.4. General procedure for the oxidation of styrene to benzaldehyde

The catalytic activity of compounds **1–4** was tested for the oxidative conversion of styrene to benzaldehyde. The catalytic experiments were performed using styrene, 30 wt% aqueous hydrogen peroxide or 70 wt% aqueous TBHP, acetonitrile, and chlorobenzene (internal standard). All reagents were p.a. and used as received.

A typical procedure is as follows. The oxidation reactions were carried out in sealed tubes with styrene (1.0 mmol), metal complex **1–4** (5 µmol), 30 wt% aqueous H<sub>2</sub>O<sub>2</sub> (4 mmol), 1.5 mL of acetonitrile and chlorobenzene as the internal standard (100 µL). The reaction mixture was stirred for 3 h at 80 °C and then analysed by gas chromatography on a FISONS Instruments GC 8000 with an FID detector and a DB-WAX capillary column (internal diameter 0.32 mm, length 30 m) using He as a carrier, with an injection temperature of 200 °C. The reaction products were identified by comparison with known reference compounds and the yield values, determined by the internal standard method, were obtained by averaging from several runs with similar results.

## Conflicts of interest

There are no conflicts to declare.

## Acknowledgements

This work was supported by the Fundação para a Ciência e a Tecnologia (FCT) (Portugal), projects UIDB/00100/2020, UIDP/00100/2020 and LA/P/0056/2020 of Centro de Química Estrutural. A. V. G. and K. T. M. thank FCT and Instituto Superior Técnico (DL 57/2016, L 57/2017 and CEEC Institutional 2018 Programs, Contracts no: IST-ID/110/2018 and IST-ID/85/2018). K. T. M. and A. V. G. acknowledge the Baku State University (Azerbaijan). The authors thank the Portuguese NMR Network (IST-UL Centre) and the IST Node of the Portuguese Network of mass-spectrometry. This work was also supported by the SOCAR Science Foundation, S/N 12LR-AMEA (05/01/2022).

## References

- (a) L. Bourget-Merle, M. F. Lappert and J. R. Severn, *Chem. Rev.*, 2002, **102**, 3031–3066; (b) R. L. Webster, *Dalton Trans.*, 2017, **46**, 4483–4498; (c) M. N. Kopylovich and A. J. L. Pombeiro, *Coord. Chem. Rev.*, 2011, **255**, 339–355; (d) K. T. Mahmudov, M. N. Kopylovich and A. J. L. Pombeiro, *Coord. Chem. Rev.*, 2013, **257**, 1244–1281.
- (a) A. Das, S. Mukhopadhyay, L.-P. Lu and M.-L. Zhu, *J. Chem. Crystallogr.*, 2006, **36**, 297–301; (b) L. Lu, M. Zhu and P. Yang, *Acta Crystallogr., Sect. C: Cryst. Struct. Commun.*, 2004, **60**, m18–m20; (c) R. O. C. Hart, S. G. Bott, J. L. Atwood and S. R. Cooper, *J. Chem. Soc., Chem. Commun.*, 1992, 894–895; (d) G. Das, P. K. Bharadwaj, D. Ghosh, B. Chaudhuri and R. Banerjee, *Chem. Commun.*, 2001, 323–324; (e) M. Zhou, Y. Song, T. Gong, H. Tong, J. Guo, L. Weng and D. Liu, *Inorg. Chem.*, 2008, **47**, 6692–6700; (f) N. Q. Shixaliyev, A. V. Gurbanov, A. M. Maharramov, K. T. Mahmudov, M. N. Kopylovich, L. M. D. R. S. Martins, V. M. Muzalevskiy, V. G. Nenajdenko and A. J. L. Pombeiro, *New J. Chem.*, 2014, **38**, 4807–4815; (g) V. Duros, H. Sartzi, S. J. Teat, Y. Sanakis, O. Roubeau and S. P. Perlepes, *Inorg. Chem. Commun.*, 2014, **50**, 117–121.
- A. Igashira-Kamiyama, T. Kajiwara, M. Nakano, T. Konno and T. Ito, *Inorg. Chem.*, 2009, **48**, 11388–11393.
- (a) C. Valdebenito, M. T. Garland, R. Quijada and R. Rojas, *J. Organomet. Chem.*, 2009, **694**, 717–725; (b) P. J. Figiel, M. N. Kopylovich, J. Lasri, M. F. C. Guedes da Silva, J. J. R. Frausto da Silva and A. J. L. Pombeiro, *Chem. Commun.*, 2010, **46**, 2766–2768; (c) A. P. C. Ribeiro, Y. Y. Karabach, L. M. D. R. S. Martins, A. G. Mahmoud, M. F. C. Guedes da Silva and A. J. L. Pombeiro, *RSC Adv.*, 2016, **6**, 29159–29163; (d) N. Y. Rad'kova, T. A. Kovylina, A. V. Cherkasov, K. A. Lyssenko, A. M. Ob'edkov and A. A. Trifonov, *Eur. J. Inorg. Chem.*, 2021, 2390–2400; (e) O. V. Nesterova, M. N. Kopylovich and D. S. Nesterov, *Inorganics*, 2019, **7**, 82; (f) N. V. Kulkarni, A. Das, S. G. Ridlen, E. Maxfield, V. A. K. Adiraju, M. Yousufuddin and H. V. R. Dias, *Dalton Trans.*, 2016, **45**, 4896–4906; (g) T. T. Ponduru, C. Qiu, J. X. Mao, A. Leghissa, J. Smuts, K. A. Schug and H. V. R. Dias, *New J. Chem.*, 2018, **42**, 19442–19449.
- Noncovalent Interactions in Catalysis*, eds. K. T. Mahmudov, M. N. Kopylovich, M. F. C. Guedes da Silva and A. J. L. Pombeiro, Royal Society of Chemistry, UK, 2019.
- (a) J. Xu, Y. Zhang, X. Yue, J. Huo, D. Xionga and P. Zhang, *Green Chem.*, 2021, **23**, 5549–5555; (b) A. Rubinstein, P. Jiménez-Lozano, J. J. Carbó, J. M. Poblet and R. Neumann, *J. Am. Chem. Soc.*, 2014, **136**, 10941–10948; (c) Y. Chang, Y. Xie, C. Zhao, J. Ren, W. Su, W. Zhao, L. Wu and H. Yu, *ChemCatChem*, 2022, **14**, e202200209.
- (a) G. Liu, M. Hou, J. Song, Z. Zhang, T. Wu and B. Han, *J. Mol. Catal. A: Chem.*, 2010, **316**, 90–94; (b) F. Bruhne and E. Wrigg, *Benzaldehyde, Ullmann's Encyclopedia of Industrial Chemistry*, 7th edn, 2011, John Wiley & Sons, NY, NY.
- M. A. Andrade and L. M. D. R. S. Martins, *Molecules*, 2021, **26**, 1680.
- (a) B. Feng, Z. Hou, X. Wang, Y. Hu, H. Lia and Y. Qiao, *Green Chem.*, 2009, **11**, 1446–1452; (b) N. S. Lawal, H. Ibrahim and M. D. Bala, *Molecules*, 2022, **27**, 4941; (c) Y. Chang, F. Zha, B. Su and Y. Wang, *J. Macromol. Sci., Part A: Pure Appl. Chem.*, 2006, **43**, 923–931; (d) M. K. Pandey, J. T. Mague and M. S. Balakrishna, *Inorg. Chem.*, 2018, **57**, 7468–7480; (e) T. A. G. Duarte, A. P. Carvalho and L. M. D. R. S. Martins, *Catal. Today*, 2020, **357**, 56–63; (f) A. Paul, L. M. D. R. S. Martins, A. Karmakar, M. L. Kuznetsov, M. F. C. Guedes da Silva and A. J. L. Pombeiro, *Molecules*, 2020, **25**, 2644–2657; (g) N. M. R. Martins, A. J. L. Pombeiro and L. M. D. R. S. Martins, *Cat. Commun.*, 2018, **116**, 10–15; (h) T. A. G. Duarte, A. P. Carvalho and L. M. D. R. S. Martins, *Catal. Sci. & Tech.*, 2018, **8**, 2285–2288.



10 Z. Ma, K. T. Mahmudov, V. A. Aliyeva, A. V. Gurbanov, M. F. C. Guedes da Silva and A. J. L. Pombeiro, *Coord. Chem. Rev.*, 2021, **437**, 213859.

11 A. W. Addison, T. N. Rao, J. Reedijk, J. van Rijn and G. C. Verschoor, *J. Chem. Soc., Dalton Trans.*, 1984, 1349–1356.

12 C. Guo, Y. Zhang, L. Zhang, Y. Guo, N. Akram and J. Wang, *ACS Appl. Nano Mater.*, 2018, **1**, 5289.

13 X. Zhu, R. Shen and L. Zhang, Catalytic oxidation of styrene to benzaldehyde over a copper Schiff-base/SBA-15 catalyst, *Chin. J. Catal.*, 2014, **35**, 1716.

14 N. S. Lawal, H. Ibrahim and M. D. Bala, *Molecules*, 2022, **27**, 4941.

15 S. R. Amanchi, A. Patel and S. K. Das, *J. Chem. Sci.*, 2014, **126**, 1641–1645.

16 SMART & SAINT Software Reference Manuals, Version 6.22, Bruker AXS Analytic X-ray Systems, Inc., Madison, WI, 2000.

17 G. M. Sheldrick, *SADABS Software for Empirical Absorption Correction*, University of Göttingen, Germany, 2000.

18 G. M. Sheldrick, *SHELXTL V5.1, Software Reference Manual*, Bruker AXS Inc., Madison, Wisconsin, 1997.

19 A. L. Spek, *J. Appl. Crystallogr.*, 2003, **36**, 7–13.

